Journal of King Saud University – Science (2017) 29, 235–240

King Saud University
Journal of King Saud University – Science
www.ksu.edu.sa
www.sciencedirect.com

ORIGINAL ARTICLE

Operational matrix approach for approximate solution of fractional model of Bloch equation

Harendra Singh

Department of Mathematical Sciences, Indian Institute of Technology, Banaras Hindu University, Varanasi 221005, India

Received 8 July 2016; accepted 10 November 2016
Available online 18 November 2016

KEYWORDS

Fractional model of Bloch equation;
Nuclear magnetic resonance;
Operational matrix of integration;
Laguerre polynomial

Abstract In present paper operational matrix of integration for Laguerre polynomial is used to solve fractional model of Bloch equation in nuclear magnetic resonance (NMR). The operational matrix converts the Bloch equation in a system of linear algebraic equations. Solving system we obtain the approximate solutions for fractional Bloch equation. Results are compared with existing methods and exact solution. Graphs are plotted for different fractional values of time derivatives.

1. Introduction

The fractional Bloch equations are used in physics, chemistry, nuclear magnetic resonance (NMR), electron spin resonance (ESR) and magnetic resonance imaging (MRI). The fractional Bloch equation is generalization of standard Bloch equation and obtained by replacing integer order time derivative to fractional order Caputo derivative. Fractional calculus has many real applications in science and engineering such as fluid-dynamic traffic (He, 1999), biology (Robinson, 1981), viscoelasticity (Bagley and Torvik, 1983a,b, 1985), signal processing (Panda and Dash, 2006), bioengineering (Magin, 2004) and control theory (Bohannan, 2008). The fractional model of Bloch equation is given as,

$$\begin{aligned}
\frac{d^{\alpha}M_x(t)}{dt^{\alpha}} &= \omega_0 M_y(t) - \frac{M_x(t)}{T_2},\\
\frac{d^{\beta}M_y(t)}{dt^{\beta}} &= -\omega_0 M_x(t) - \frac{M_y(t)}{T_2},\\
\frac{d^{\gamma}M_z(t)}{dt^{\gamma}} &= \frac{M_0 - M_z(t)}{T_1},
\end{aligned} \tag{1}$$

where $0 < \alpha, \beta, \gamma \leqslant 1$, with initial conditions $M_x(0) = 0$, $M_y(0) = 100$ and $M_z(0) = 0$.

Where $M_x(t), M_y(t)$ and $M_z(t)$ represent the system magnetization in x, y and z component respectively, M_0 is the equilibrium magnetization, ω_0 is the resonant frequency given by theLarmor relationship $\omega_0 = \gamma B_0$, where B_0 is the static magnetic field in z -component, T_1 is spin-lattice relaxation time, T_2 is spin-spin relaxation time. The set of analytical solutions for integer order Bloch equation is given as,

$$\begin{aligned}
M_x(t) &= e^{-t/T_2}(M_x(0)\cos\omega_0 t + M_y(0)\sin\omega_0 t),\\
M_y(t) &= e^{-t/T_2}(M_y(0)\cos\omega_0 t - M_x(0)\sin\omega_0 t),\\
M_z(t) &= M_z(0)e^{-t/T_1}M_0(1 - e^{-t}/T_1).
\end{aligned} \tag{2}$$

The fraction in time derivative suggests a modulation—or weighting—of system memory (West et al., 2003; Magin et al., 2008), the assumption of fractional derivatives plays an important role affecting the spin dynamics described by the Bloch equations in Eq. (1). More recently, time fractional

E-mail addresses: harendra059@gmail.com, harendrasingh.rs.apm12@iitbhu.ac.in
Peer review under responsibility of King Saud University.

Production and hosting by Elsevier

http://dx.doi.org/10.1016/j.jksus.2016.11.001
1018-3647

model of Bloch equation was resolved using Homotopy perturbation method (Kumar et al., 2014) and Petráš (2011) used iterative method to solve fractional model of Bloch equation. A generalization of the fractional Bloch equation by taking delay in the time was reported through numerical solution (Bhalekar et al., 2011). Recently Yu et al. (2014), gave an implicit numerical method to solve fractional Bloch equation in NMR. Some other existing methods to solve Bloch equation in NMR are reported in the literature (Hoult, 1979; Sivers, 1986; Yan et al., 1987; Xu and Chan, 1999; Balac and Chupin, 2008; Magin et al., 2009; Murase and Tanki, 2011; Sun et al., 2016). In this paper we are using operational matrix of fractional integration of Laguerre polynomial to solve fractional model of Bloch equation as Laguerre polynomials are more convenient for computational purpose. Recent investigations report the application of operational matrices to solve fractional differential equations (Wu, 2009; Yousefi et al., 2011; Kazem et al., 2013; Tohidi et al., 2013; Heydari et al., 2014; Zhou and Xu, 2014; Bhrawy and Zaky, 2015; Singh and Singh, 2016). Using operational matrix we convert the Bloch equation into a system of linear algebraic equation whose solution gives approximate solution for Bloch equation in NMR.

2. Preliminaries and operational matrix

In this paper, the fractional order differentiations and integrations are in well-known Caputo and Riemann-Liouville sense respectively (Miller and Ross, 1993; Diethelm et al., 2005).

Definition 2.1. The Riemann-Liouville fractional order integral operator is given by

$$I^{\alpha}f(x) = \frac{1}{\lceil\alpha} \int_0^x (x-t)^{\alpha-1} f(t)dt \quad \alpha > 0, \quad x > 0,$$

$$I^0 f(x) = f(x).$$

Definition 2.2. The Caputo fractional derivative of order β are defined as

$$D^{\beta}f(x) = I^{m-\beta}D^m f(x) = \frac{1}{\lceil(m-\beta)} \int_0^x (x-t)^{m-\beta-1} \frac{d^m}{dt^m} f(t)dt,$$

$$m-1 < \beta < m, \quad x > 0.$$

The Laguerre polynomial is defined by Ali et al. (2015) and Bhrawy et al. (2014)

$$L_k(t) = \sum_{i=0}^{k} \frac{(-1)^i}{i!} \binom{k}{i} t^i, \quad k = 0, 1, 2, \ldots, n. \tag{3}$$

The set of Laguerre polynomial $\{L_0(t), L_1(t), \ldots, L_n(t)\}$ forms an orthonormal basis with respect to weight function $w(t) = e^{-t}$ on the interval $[0, \infty)$ with the following property,

$$\int_0^{\infty} L_i(t)L_j(t)w(t)dt = \delta_{ij}, \quad \forall i,j \geqslant 0, \tag{4}$$

where δ_{ij} is the kronecker delta function.

A function $f(t)$, square integrable in $[0, \infty)$ may be expressed as sum of Laguerre polynomial as follows:

$$f(t) = \lim_{n\to\infty} \sum_{i=0}^{n} c_i L_i(t), \tag{5}$$

where $c_i = \int_0^{\infty} f(t)w(t)L_i(t)dt$.

If the series is truncated at $n = m$, then we have

$$f \cong \sum_{i=0}^{m} c_i L_i = F^T \psi(t), \tag{6}$$

where F and $\psi(t)$ are $(m+1) \times 1$ matrices given by,

$$F = [c_0, c_1, \ldots, c_m]^T \quad \text{and} \quad \psi(t) = [L_0(t), L_1(t), \ldots, L_m(t)]^T.$$

Theorem 2.1. *Let* $\psi(t) = [L_0(t), L_1(t), \ldots, L_n(t)]^T$, *be Laguerre vector and consider* $\alpha > 0$, *then*

$$I^{\alpha}L_i(t) = I^{(\alpha)}\psi(t), \tag{7}$$

where $I^{(\alpha)} = (\theta(i,j))$, is $(n+1) \times (n+1)$ *operational matrix of fractional integral of order* α *and its* (i,j) *th entry is given by*

$$\theta(i,j) = \sum_{k=0}^{i}\sum_{r=0}^{j} (-1)^{k+r} \frac{i!r!\Gamma(k+\alpha+r+1)}{(i-k)!(k)!(j-r)!(r!)^2\Gamma(\alpha+k+1)}$$

$$0 \leqslant i,j \leqslant n. \tag{8}$$

Proof. Pl see (Bhrawy and Taha, 2012). □

3. Outline of method

In this section, we describe the outline of the method for the construction of approximate solution of the Bloch equation.

Consider the following approximations:

$$\frac{d^{\alpha}M_x(t)}{dt^{\alpha}} = F_1^T\psi(t), \quad \frac{d^{\beta}M_y(t)}{dt^{\beta}} = F_2^T\psi(t), \quad \frac{d^{\gamma}M_z(t)}{dt^{\gamma}} = F_3^T\psi(t). \tag{9}$$

Taking integral of order α, β and γ in component M_x, M_y and M_z respectively in Eq. (9) we get,

$$M_x(t) = F_1^T I^{(\alpha)}\psi(t) + M_x(0), \tag{10}$$

$$M_y(t) = F_2^T I^{(\beta)}\psi(t) + M_y(0), \tag{11}$$

$$M_z(t) = F_3^T I^{(\gamma)}\psi(t) + M_z(0). \tag{12}$$

Let

$$M_x(0) = P^T\psi(t), \quad M_y(0) = Q^T\psi(t), \quad M_z(0) = R^T\psi(t). \tag{13}$$

From Eqs. (10)–(13) we get,

$$M_x(t) = (F_1^T I^{(\alpha)} + P^T)\psi(t), \tag{14}$$

$$M_y(t) = (F_2^T I^{(\beta)} + Q^T)\psi(t), \tag{15}$$

$$M_z(t) = (F_3^T I^{(\gamma)} + R^T)\psi(t). \tag{16}$$

Using Eqs. (9), (14), (15) and (16) in Eq. (1) we get following equations,

$$F_1^T\left(I+\frac{1}{T_2}I^{(\alpha)}\right)-\omega_0F_2^TI^{(\beta)}=\omega_0Q^T-\frac{1}{T_2}P^T, \quad (17)$$

$$\omega_0F_1^TI^{(\alpha)}+F_2^T\left(I+\frac{1}{T_2}I^{(\beta)}\right)=-\omega_0P^T-\frac{1}{T_2}Q^T, \quad (18)$$

$$F_3^T\left(I+\frac{1}{T_1}I^{(\gamma)}\right)=S^T-\frac{1}{T_1}R^T, \quad (19)$$

where $\frac{M_0}{T_1}=S^T\psi(t)$ and $I^{(\alpha)}, I^{(\beta)}, I^{(\gamma)}$ are operational matrices of fractional integration of order α, β and γ respectively. I is an identity matrix.

On solving Eqs. (17) and (18) we get,

$$F_1^T=\left(\left(\omega_0Q^T-\frac{1}{T_2}P^T\right)(\omega_0I^{(\beta)})^{-1}+\left(-\omega_0P^T-\frac{1}{T_2}Q^T\right)\left(I+\frac{1}{T_2}I^{(\beta)}\right)^{-1}\right)\times\left(\left(I+\frac{1}{T_2}I^{(\alpha)}\right)(\omega_0I^{(\beta)})^{-1}+(\omega_0I^{(\alpha)})\left(I+\frac{1}{T_2}I^{(\beta)}\right)^{-1}\right)^{-1}, \quad (20)$$

$$F_2^T=\left\{\left(\left(\omega_0Q^T-\frac{1}{T_2}P^T\right)(\omega_0I^{(\beta)})^{-1}+\left(-\omega_0P^T-\frac{1}{T_2}Q^T\right)\left(I+\frac{1}{T_2}I^{(\beta)}\right)^{-1}\right)\times\left(\left(I+\frac{1}{T_2}I^{(\alpha)}\right)(\omega_0I^{(\beta)})^{-1}+(\omega_0I^{(\alpha)})\left(I+\frac{1}{T_2}I^{(\beta)}\right)^{-1}\right)^{-1}\left(I+\frac{1}{T_2}I^{(\alpha)}\right)-\left(\omega_0Q^T-\frac{1}{T_2}P^T\right)\right\}(\omega_0I^{(\beta)})^{-1}. \quad (21)$$

From Eq. (19), we can write

$$F_3^T=\left(S^T-\frac{1}{T_1}R^T\right)\left(I+\frac{1}{T_1}I^{(\gamma)}\right)^{-1}, \quad (22)$$

Using Eqs. (20)–(22) in Eqs. (14)–(16) respectively, we get approximate solution for Bloch equations in NMR.

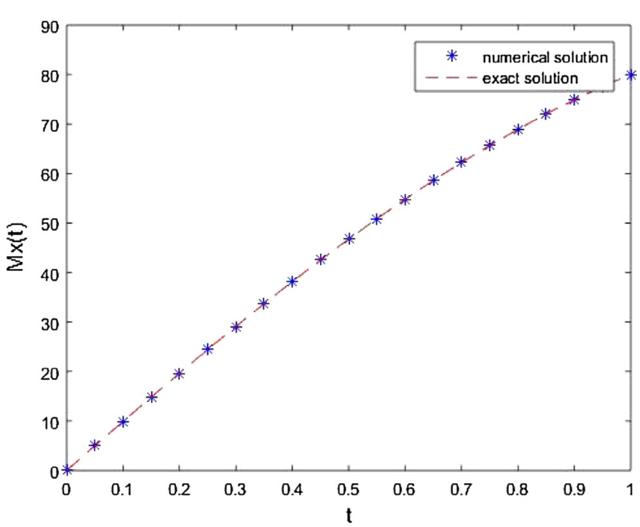

Figure 1 Comparison of exact and approximate solution for $M_x(t)$ at n = 15.

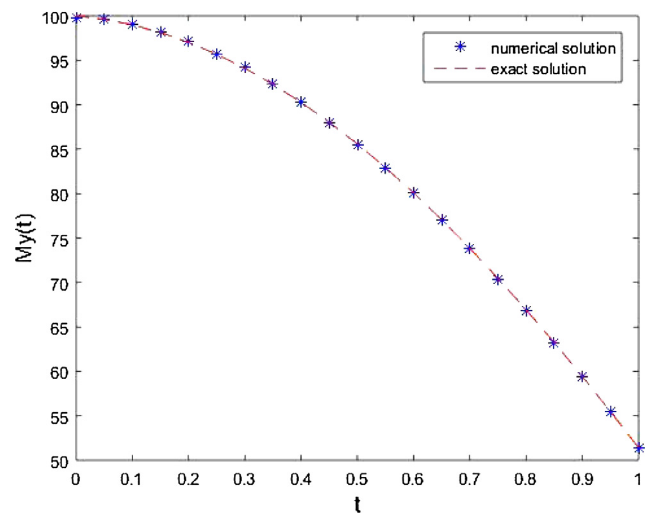

Figure 2 Comparison of exact and approximate solution for $M_y(t)$ at n = 15.

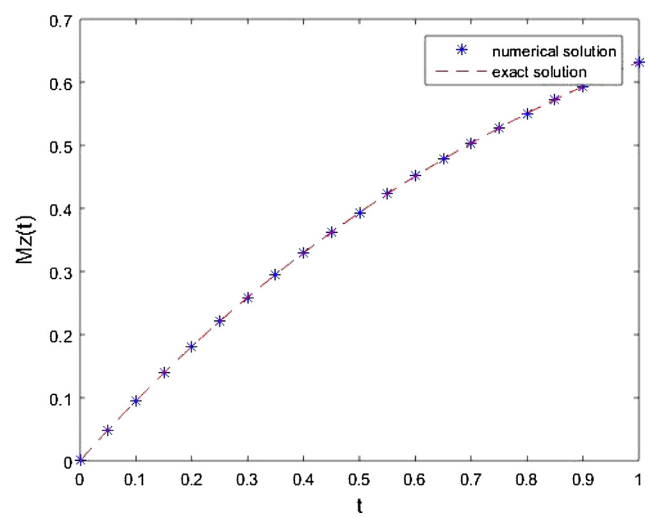

Figure 3 Comparison of exact and approximate solution for $M_z(t)$ at n = 15.

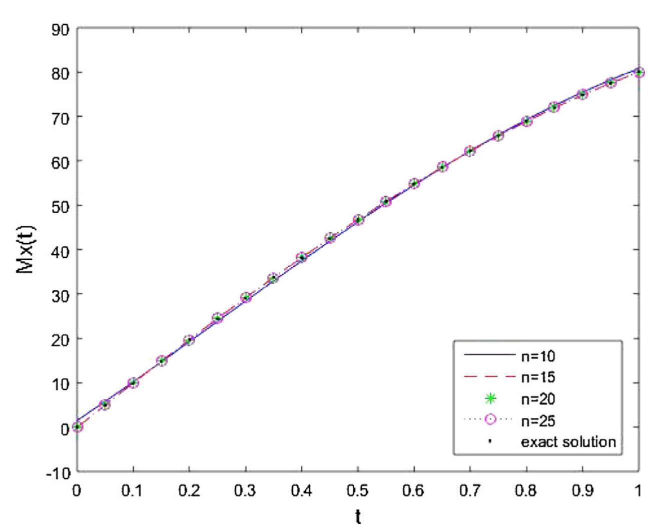

Figure 4 Comparison of approximate solution at different values of n = 10, 15, 20, 25 and exact solution for $M_x(t)$.

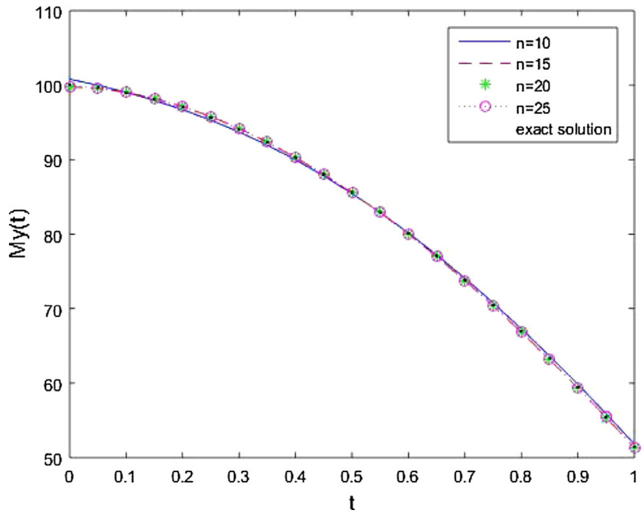

Figure 5 Comparison of approximate solution at different values of n = 10, 15, 20, 25 and exact solution for $M_y(t)$.

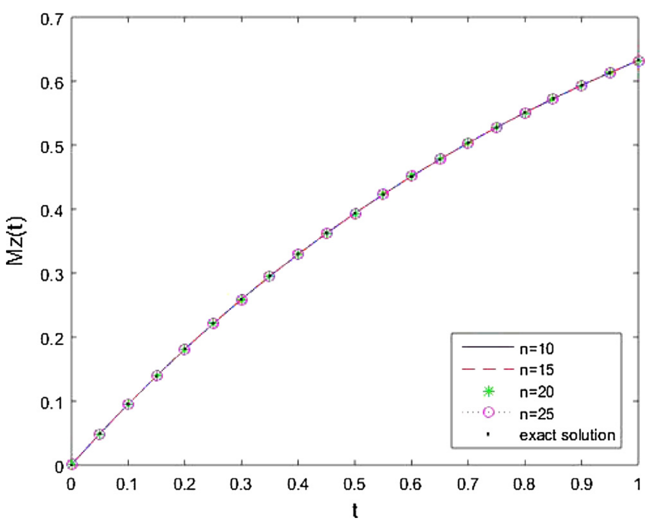

Figure 6 Comparison of approximate solution at different values of n = 10, 15, 20, 25 and exact solution for $M_z(t)$.

4. Numerical results and discussion

In all the figures given below we have taken $\omega_0 = 1$, $T_1 = 1\,(s)^q$ and $T_2 = 20\,(ms)^q$.

Figs. 1–3, represent comparison of exact and approximate solution for $M_x(t), M_y(t)$ and $M_z(t)$ at n = 15 respectively.

Figs. 4–6, show the behaviour of approximate solutions at values of n = 10, 15, 20, 25 and exact solution for $M_x(t)$, $M_y(t)$ and $M_z(t)$ respectively. From Figs. 4–6, it is observed that approximate solution comes close to the exact solution with the increasing n.

The behaviour of approximate solutions with time for different values of fractional order time derivatives α, β and γ is shown from Figs. 7–9, respectively. It is clear that the solution varies continuously with fractional values of time derivatives

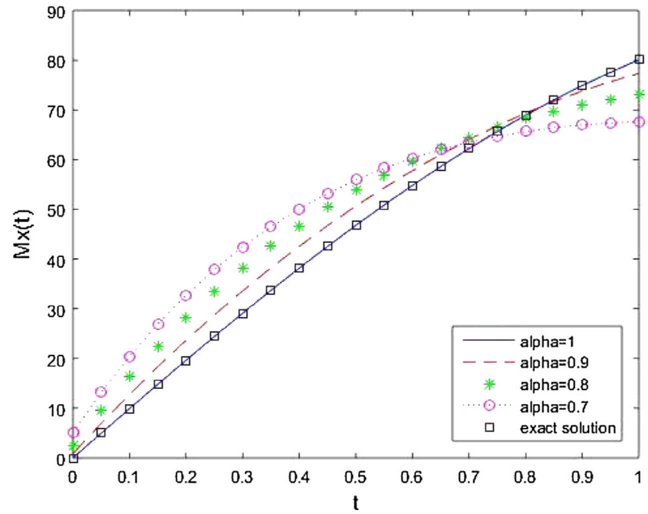

Figure 7 Approximate solution for $M_x(t)$ at different values of α and exact solution.

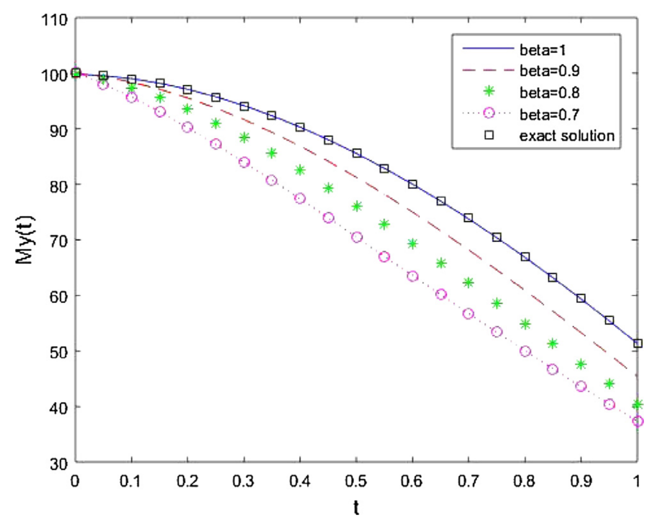

Figure 8 Approximate solution for $M_y(t)$ at different values of β and exact solution.

for fractional Bloch equation in NMR and for $\alpha = \beta = \gamma = 1$ solution for standard Bloch equation is obtained. In Figs. 7 and 9 the approximate solution for $M_x(t)$ and $M_z(t)$ increases with the increasing of time for different value of $\alpha = \gamma = 0.7.0.8, 0.9$ and 1. In Fig. 8 the approximate solution for $M_y(t)$ decreases with the increasing of time for different value of $\beta = 0.7.0.8, 0.9$ and 1.

To show the accuracy of the proposed method we have compared our results from existing methods and exact solution. In Table 1 comparison of our results from the Homotopy Perturbation Method (HPM) (Kumar et al., 2014), iterative method (Petráš, 2011) and exact solution is given.

In Table 2, we have listed maximum absolute errors and root mean square errors of $M_x(t), M_y(t)$ and $M_z(t)$ for different values of n = 15, 20.

From Table 2, it is clear that as the value of n increases maximum absolute errors and root mean square decreases.

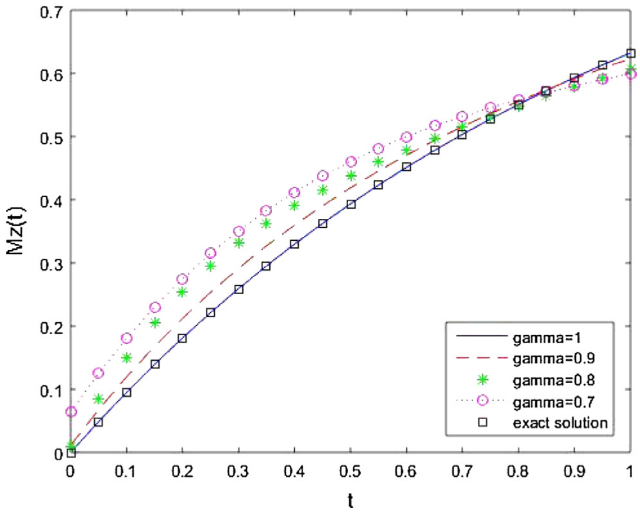

Figure 9 Approximate solution for $M_z(t)$ at different values of γ and exact solution.

Table 1 Comparison among the approximate solutions of exiting methods, present method and exact solution for $M_x(t), M_y(t) and M_z(t)$.

M	t	Exact solution	Present method	Kumar et al. (2014)	Petráš (2011)
$M_x(t)$	0.1	9.9335	9.9245	9.9335	9.2237
	0.3	29.1120	29.1080	29.1034	29.0937
	0.5	46.7588	46.7732	46.6823	46.7507
	0.7	62.2060	62.2180	61.8762	62.1921
	0.9	74.8859	74.8814	73.8911	74.8806
$M_y(t)$	0.1	99.0042	99.0213	99.0187	99.0051
	0.3	94.1113	94.1645	94.1837	94.1166
	0.5	85.5915	85.5689	85.5518	85.5942
	0.7	73.8536	73.7886	73.1630	73.8635
	0.9	59.4258	59.3782	57.0572	59.4296
$M_z(t)$	0.1	0.0952	0.0952	0.0952	0.0952
	0.3	0.2592	0.2592	0.2592	0.2590
	0.5	0.3935	0.3935	0.3935	0.3934
	0.7	0.5034	0.5034	0.5034	0.5033
	0.9	0.5934	0.5934	0.5934	0.5934

Table 2 Comparisons of MAE and RMSE for $M_x(t), M_y(t)$ and $M_z(t)$ at different values of n.

M	n	Maximum absolute error (MAE)	Root mean square error (RMSE)
$M_x(t)$	1.5	1.3010×10^{-1}	1.9548×10^{-2}
	20	2.3951×10^{-2}	3.8708×10^{-3}
$M_y(t)$	1.5	2.4869×10^{-1}	2.4727×10^{-2}
	20	1.77996×10^{-1}	1.7752×10^{-2}
$M_z(t)$	1.5	1.6746×10^{-5}	2.2963×10^{-6}
	20	1.1466×10^{-5}	1.5568×10^{-6}

In Table 3, we have listed root mean square at different points from our method and Homotopy Perturbation Method (HPM) (Kumar et al., 2014), iterative method (Petráš, 2011).

Table 3 Comparison among the absolute errors of exiting methods and present method for $M_x(t), M_y(t) and M_z(t)$.

M	t	Present Method	Kumar et al. (2014)	Petráš (2011)
$M_x(t)$	0.2	1.1300×10^{-2}	1.6000×10^{-2}	9.5100×10^{-2}
	0.4	9.1000×10^{-3}	2.9400×10^{-2}	8.6600×10^{-2}
	0.6	1.5200×10^{-2}	1.6850×10^{-1}	7.4800×10^{-2}
	0.8	1.8000×10^{-3}	5.9210×10^{-1}	6.0500×10^{-2}
	1.0	1.6200×10^{-2}	1.5849	4.4200×10^{-2}
$M_y(t)$	0.2	7.9300×10^{-2}	4.6800×10^{-2}	1.1460×10^{-2}
	0.4	2.2400×10^{-2}	5.7600×10^{-2}	2.3200×10^{-2}
	0.6	6.0300×10^{-2}	2.6970×10^{-1}	3.0500×10^{-2}
	0.8	7.7300×10^{-2}	1.3665	3.6400×10^{-2}
	1.0	3.2500×10^{-2}	3.7682	4.0500×10^{-2}
$M_z(t)$	0.2	5.0663×10^{-6}	2.0000×10^{-6}	7.3754×10^{-4}
	0.4	5.6125×10^{-7}	9.8900×10^{-5}	5.3672×10^{-4}
	0.6	4.1742×10^{-6}	3.0000×10^{-6}	3.8447×10^{-4}
	0.8	4.1005×10^{-6}	1.0002×10^{-6}	2.6978×10^{-4}
	1.0	6.3039×10^{-7}	1.2000×10^{-6}	1.8405×10^{-4}

Table 4 Computational order obtained for $M_x(t), M_y(t) and M_z(t)$.

M	n	E_n	Computational order
$M_x(t)$	5	10.71300	–
	10	1.49014	2.8458
	20	2.39506×10^{-2}	5.9592
$M_y(t)$	5	2.784942	–
	10	0.82201	1.7604
	20	1.77996×10^{-1}	2.2073
$M_z(t)$	5	0.01563	–
	10	4.88281×10^{-4}	5.0000
	20	1.14664×10^{-5}	5.4122

The computational order for the numerical results are given as (Dehghan et al., 2015; Singh and Singh, 2016)

Order $= \log_2\left[\frac{E_n}{E_{2n}}\right]$ where E_n is maximum absolute error ($\max_{1\leqslant i\leqslant N} E(x_i)$) for approximation having n number of basis elements.

In Table 4, we list the computational order for the numerical results.

From Table 4, it is clear that our method is good for computational purposes in comparison to iterative method (Petráš, 2011) in which we take thousands of iterations to achieve the desired accuracy.

5. Conclusions

Our method is easy for computation purposes because we are approximating time derivatives first. Our numerical algorithm is easy to implement in compare to existing methods because construction of operational matrix is very easy. It is presented how the approximate solution varies continuously for different values of fractional time derivatives and for integer order approximate solution coinciding with the exact solution for Bloch equation.

Acknowledgements

The author acknowledges the financial support from Ministry of Human Resource Development, Indian Institute of Technology, Banaras Hindu University, Varanasi, India under the SRF scheme. The author is very grateful to the referees for their constructive comments and suggestions for the improvement of the paper.

References

Ali, A., Salahshour, S., Baleanu, D., Amirkhani, H., Yunus, R., 2015. Tau method for the numerical solution of a fuzzy fractional kinetic model and its application to the Oil Palm Frond as a promising source of xy lose. J. Comput. Phys. 294, 562–584.

Bagley, R.L., Torvik, P.J., 1983a. A theoretical basis for the application of fractional calculus to viscoelasticity. J. Rheol. 27, 201–210.

Bagley, R.L., Torvik, P.J., 1983b. Fractional calculus a differential approach to the analysis of viscoelasticity damped structures. AIAA J. 21 (5), 741–748.

Bagley, R.L., Torvik, P.J., 1985. Fractional calculus in the transient analysis of viscoelasticity damped structures. AIAA J. 23, 918–925.

Balac, S., Chupin, L., 2008. Fast approximate solution of Bloch equation for simulation of RF artifacts in Magnetic Resonance Imaging. Math. Comput. Model. 48, 1901–1913.

Bhalekar, S., Daftardar-Gejji, V., Baleanu, D., Magin, R., 2011. Fractional Bloch equation with delay. Comput. Math. Appl. 61 (5), 1355–1365.

Bhrawy, A.H., Taha, T.M., 2012. An operational matrix of fractional integration of the Laguerre polynomials and its application on a semi-infinite interval. Math. Sci. 6, 41.

Bhrawy, A.H., Zaky, M.A., 2015. A method based on Jacobi tau approximation for solving multi-term time-space fractional partial differential equations. J. Comput. Phys. 281, 876–895.

Bhrawy, A.H., Alhamed, Y.A., Baleanu, D., Al-Zahrani, A.A., 2014. New spectral techniques for systems of fractional differential equations using fractional-order generalized Laguerre orthogonal functions. Fract. Calc. Appl. Anal. 17, 1137–1157.

Bohannan, G.W., 2008. Analog fractional order controller in temperature and motor control applications. J. Vib. Control 14, 1487–1498.

Dehghan, M., Abbaszadeh, M., Mohebbi, A., 2015. Error estimate for the numerical solution of reaction-sub diffusion process based on a mesh less method. J. Comput. Appl. Math. 280 (15), 14–36.

Diethelm, K., Ford, N.J., Freed, A.D., Luchko, Y., 2005. Algorithms for fractional calculus: a selection of numerical methods. Comput. Methods Appl. Mech. Eng. 194, 743–773.

He, J.H., 1999. Some applications of nonlinear fractional differential equations and their approximations. Bull. Sci. Technol. 15 (2), 86–90.

Heydari, M.H., Hooshmandasl, M.R., Ghaini, F.M.M., 2014. A new approach of the Chebyshev wavelets method for partial differential equations with boundary conditions of the telegraph type. Appl. Math. Model. 38, 1597–1606.

Hoult, D.I., 1979. The solution of the Bloch equation in presence of varying B 1 field – An approach to selective pulse analysis. J. Magn. Reson. 35, 69–86.

Kazem, S., Abbasbandy, S., Kumar, S., 2013. Fractional order Legendre functions for solving fractional-order differential equations. Appl. Math. Model. 37, 5498–5510.

Kumar, S., Faraz, N., Sayevand, K., 2014. A fractional model of Bloch equation in NMR and its analytic approximate solution. Walailak J. Sci. Technol. 11 (4), 273–285.

Magin, R.L., 2004. Fractional calculus in bioengineering. Crit. Rev. Biomed. Eng. 32, 1–104.

Magin, R.L., Abdullah, O., Baleanu, D., Zhou, X.J., 2008. Anomalous diffusion expressed through fractional order differential operators in the Bloch-Torrey equation. J. Magn. Reson. 190, 255–270.

Magin, R., Feng, X., Baleanu, D., 2009. Solving the fractional order Bloch Equation. Wiley Inter Sci. 34 A (1), 16–23.

Miller, K., Ross, B., 1993. An introduction to fractional calculus and fractional differential equations. John Wiley & Sons Inc, New York.

Murase, K., Tanki, N., 2011. Numerical solution to the time dependent Bloch equations revisited. J. Magn. Reson. 29, 126–131.

Panda, R., Dash, M., 2006. Fractional generalized splines and signal processing. Signal process 86, 2340–2350.

Petráš, I., 2011. Modeling and numerical analysis of fractional-order Bloch equations. Comput. Math. Appl. 61, 341–356.

Robinson, A.D., 1981. The use of control systems analysis in neurophysiology of eye movements. Ann. Rev. Neurosci. 4, 462–503.

Singh, H., Singh, C.S., 2016. Stable numerical solutions of fractional partial differential equations using Legendre scaling functions operational matrix. Ain Shams Eng. J. http://dx.doi.org/10.1016/j.asej.2016.03.013.

Sivers, E.A., 1986. Approximate solution to the Bloch equation with symmetric RF pulses and flip angles less than TT/2. J. Magn. Reson. 69, 28–40.

Sun, H., Sun, Z., Gao, G., 2016. Some high order difference schemes for the space and time fractional Bloch-Torrey equations. Appl. Math. Comput. 281, 356–380.

Tohidi, E., Bhrawy, A.H., Erfani, K., 2013. A collocation method based on Bernoulli operational matrix for numerical solution of generalized pantograph equation. Appl. Math. Model. 37, 4283–4294.

West, B.J., Bolgona, M., Grigolini, P., 2003. Physics of Fractal Operators. Springer-Verlag, New York.

Wu, J.L., 2009. A wavelet operational method for solving fractional partial differential equations numerically. Appl. Math. Comput. 214, 31–40.

Xu, Z., Chan, A.K., 1999. A near-resonance solution to the Bloch equations and its application to RF pulse design. J. Magn. Reson. 138, 225–231.

Yan, H., Chen, B., Gore, J.C., 1987. Approximate solutions of the Bloch equations for selective excitation. J. Magn. Reson. 75, 83–95.

Yousefi, S.A., Behroozifar, M., Dehghan, M., 2011. The operational matrices of Bernstein polynomials for solving the parabolic equation subject to the specification of the mass. J. Comput. Appl. Math. 235, 5272–5283.

Yu, Q., Liu, F., Turner, I., Burrage, K., 2014. Numerical simulation of the fractional Bloch equations. J. Comput. Appl. Math. 255, 635–651.

Zhou, F., Xu, X., 2014. Numerical solution of convection diffusions equations by the second kind Chebyshev wavelets. Appl. Math. Comput. 247, 353–367.